Transactions of the Nigerian Association of Mathematical Physics
Volume 1, (November, 2015), pp 51 – 58

Modeling the Geometric Properties and Homo-Lumo Energy Band Gap of the Molecule Anthracene

[1]Chifu E. Ndikilar, [2]L.S. Taura, [1]Sabiu Said A and [3]Geh W. Ejuh

[1]Physics Department, Federal University Dutse, Nigeria,
[2]Physics Department, Bayero University Kano, Nigeria, (On secondment as: Dean, Faculty of Natural and Applied Sciences, Jigawa State University Kafin Hausa)
[3]University of Dschang, IUT Bandjoun, Cameroon, Department of General and Scientific Studies, P.M.B 134, Bandjoun.

Abstract

The molecular geometry (optimized bond lengths and angles) of Anthraceneis examined using ab- initio Quantum Chemical calculations at the Restricted Hartree-Fock (RHF) level of theory by employing four medium size basis sets. Density functional calculations at the Becke3LYP (B3LYP) are carried out using the same basis sets for inclusion of electron correlation. The energy band gap in each case is obtained from the computation of the energies of the Highest Occupied Molecular Orbital (HOMO) and the Lowest Unoccupied Molecular Orbital (LUMO). At all levels of theory, the band gap energies are less than one, thus showing that the molecule is a very good semi-conductor material. Inclusion of electron correlation increases the values of the band gap. The B3LYPvalues are in agreement with the experimental values.

Keywords: RHF, DFT, LUMO, HUMO, Anthracene, semiconductor.

1.0 Introduction

Anthracene has been identified as an organic semiconductor. It is a solid polycyclic aromatic compound consisting of three fused benzene rings. Typical current carriers in organic semiconductors are holes and electrons in π bonds. Almost all organic solids are insulators, but when their constituent molecules have π conjugate systems, electrons can move via π-electron cloud overlaps, especially by hopping, tunnelling and related mechanisms [1].

Conjugated polymers like Anthraceneare vital in the development of future electronic devices. Their small size, easy processing and tunable optical gaps give them an added advantage over the conventional inorganic semiconductors. Having a better understanding of the relationship between the chemical structure of this molecule and its conduction properties is important. The main factor that determines the intrinsic properties of molecules are their band structures; particularly the positions of the conduction and valence bands and the gap between them[2, 3]. In this study, we use various medium size basis sets to study the band gap of anthracene at the RHF and DFT levels of theory.

2.0 Theoretical Background

The quantitative foundations of molecular electronic energy transfer in 1946 using semi-classical quantum approach [4]. A full classical model of energy transfer is nevertheless of relevance, as it allows describing in a relatively simple and unified way radiation and non-radiation transfer, and also permits getting a deeper understanding of the underlying mechanisms of molecular conduction. Electronic energy transfer between two molecules is viewed in classical terms as the interaction of two oscillating electric dipoles. The donor's dipole is initially in oscillation, and the acceptor's dipole is initially at rest. Owing to the resonance condition, the excitation energy is progressively transferred from the first dipole to the second one. In quantum mechanics, the transfer occurs suddenly and randomly, implying that the classical result must be seen as a statistical average, either for a large ensemble of donor-acceptor pairs, or for repeated measurements performed on a single pair[4,5].

Corresponding author: Chifu E. Ndikilar, E-mail: ebenechifu@yahoo.com, Tel.: +2348069553173

The electric field of a dipole oscillating in a vacuum is given by

$$E(r,t)=\frac{p(t')}{4\pi\varepsilon_o}\left\{\left[3(n.d)n-d\right]\left(\frac{1}{r^3}-\frac{ik}{r^2}\right)+\left[(n.d)n-d\right]\frac{k^2}{r}\right\} \quad (2.1)$$

Where $p(t)$ is the time-dependent electric dipole, with amplitude p_0, $t' = t - r/c$, n is the unit vector along the donor-acceptor direction, $d$is the donor's dipole vector, k is ω/c(with $\omega = 2\pi\nu$) and r is the distance from the dipole. The distance dependence of the electric field defines two different zones. For $r \ll \lambda$ (near zone) the term in r^{-3}dominates, the angular dependence is identical to that of a static dipole, with transverse and longitudinal components; for $r \gg \lambda$ (radiation or wave zone) the r^{-1} term dominates the electric field and is always perpendicular to n (transverse field) and the radiation corresponds to a spherical wave.

The power radiated by the dipole is given [6] as:

$$p=\frac{p_0^2\omega^4}{12\pi\varepsilon_0 c^3} \quad (2.2)$$

From equation (2.2) it is seen that the radiated power is proportional to the fourth power of the frequency. For the purposes of calculating the transfer rate, the acceptor can be considered a passive absorber characterized by an absorption cross section. The power it absorbs, when placed at a distance r from the dipole [6] is

$$p'=\frac{1}{2}c\varepsilon_0 \mathrm{E}_0^2\sigma \quad (2.3)$$

where σ is the acceptor's absorption cross section and E_0 is the amplitude of the dipole's electric field. Using equation (2.1) and after orientational averaging the square of E_0can be obtained as

$$E_0^2=2\left(\frac{p_0}{4\pi\varepsilon_0}\right)^2\left(\frac{k^4}{3r^2}+\frac{k^2}{3r^4}+\frac{1}{r^6}\right) \quad (2.4)$$

Substitution of equation (2.4) into equation (2.3) gives

$$p'=\frac{\sigma}{4\pi r^2}\left[1+\left(\frac{\lambda\!\!\!^{-}}{r}\right)^2+3\left(\frac{\lambda\!\!\!^{-}}{r}\right)^4\right]p \quad (2.5)$$

Where $\lambda\!\!\!^{-}=\lambda/2\pi$. For large distances, $r \gg \lambda$, equation (2.5) reduces to

$$p'=\frac{\sigma}{4\pi r^2}p \quad (2.6)$$

Equation (2.6) shows that the power emitted and absorbed admits a simple geometric interpretation and corresponds to radiative transfer. However, equation (2.5) implies that the power emitted by the donor in the presence of an acceptor is

$$p'=\left\{1+\frac{6}{4\pi r^2}\left[\left(\frac{\lambda\!\!\!^{-}}{r}\right)^2+3\left(\frac{\lambda\!\!\!^{-}}{r}\right)^4\right]\right\}p \quad (2.7)$$

Consequently, when the acceptor is located at $r \ll \lambda$, p' exceeds p. A passive absorber can increase the donor's decay rate based on the fact that equation (2.2)refers to a time average. Using the time-dependent equation (2.1)allows one to show that energy is stored in the near field. This energy will periodically flow out from the source and return to it, without ever being lost. This energy does not appear in the net radiative balance that only accounts for the comparatively small amount of energy leaking as radiation. When an acceptor is present in the near zone, however, it feeds on the energy temporarily deposited in the field, and consequently increases the decay rate of the donor [6].

When the acceptor is in the near zone, the absorbed power is,

$$p'=\frac{3\sigma\lambda^4}{64\pi^5 r^6}p \quad (2.8)$$

Dividing both sides of equation (2.8) by $h\nu$, converts p' into the transfer rate k_T and p into the radiation constant k_r, and relating σ with the molar absorption coefficient, and the wavelength in a medium with the wavelength in a vacuum (division of the wavelength in a vacuum by the refractive index n), the rate constant for transfer in a non-absorbing medium with refractive index n is obtained [5,6] as;

$$k_T=k_r\left(\frac{3\ln 10\varepsilon\lambda^4}{64\pi^5 N_a n^4 r^6}\right) \quad (2.9)$$

$k_r$interpreted as the radiation constant of the real molecular emitter, not necessarily that of the model classical dipole. Assuming a spectral distribution for the emission wavelength and using the relation between radiation constant, fluorescence quantum yield (Φ_F^0), and fluorescence lifetime, τ_0 (in the absence of acceptor),

$$k_r = \Phi_F^0 / \tau_0 \tag{2.10}$$

The rate constant becomes,

$$k_T = \frac{1}{\tau_0}\left(\frac{3\ln 10\Phi_F^0}{64\pi^5 N_a n^4 r^6}\right)\int_0^\infty F_D(\lambda)\varepsilon(\lambda)\lambda^4 d\lambda = \frac{1}{\tau_0}\left(\frac{R_0}{r}\right)^6 \tag{2.11}$$

Where R_0 is the (isotropic) critical or Förster radius

Also, the difference between the Highest Occupied Molecular Orbital (HUMO) and the Lowest Unoccupied Molecular Orbital (LUMO) energy levels in a polymer or organic molecule is its band gap (Eg) in electron volts [3].

$$Eg = E_{LUMO} - E_{HOMO} \tag{2.12}$$

Equation (2.12) depicts that the electrical conductivity of a molecule is directly related to the HOMO and LUMO energies of the molecule.

3.0 Computational Methodology

All computations were done using Windows version of Gaussian 03 Revision C.02 software [7]. The molecular structures and geometries of anthraceneis completely optimized using ab- initio quantum mechanical calculations at the Restricted Hartree-Fock (RHF) level of theory without using any symmetry constraints using various medium sized basis sets. The structures are then refined further using Density Functional Theory which is a cost effective method for inclusion of electron correlations with the three-parameter density functional generally known as Becke3LYP (B3LYP) [8,9].

In Gaussian, a geometry optimization begins at the molecular structure specified at the input and steps along the potential energy surface. It computes the energy and gradient at that point, and determines which direction to make the next step. The gradient indicates the direction along the surface in which the energy decreases most rapidly from the current point as well as the steepness of that slope. The optimized parameters are the bond lengths (in Armstrong), the bond angles and the dihedral angles for the optimized molecular structure. Atoms in the molecule are numbered according to their order in the molecule specification section of the input.

4.0 Results and Discussion

4.1 Optimized Molecular Structure

The optimized bond lengths of Anthracene for various basis sets in gas phase are listed in Table 1.

Table 1: Optimized Bond Lengths (Å) of Anthracene

Bond	**RHF**				**B3LYP**			
	6-31G[10]	**6-31G(d)**	**6-31+G**	**6-31G(d,p)**	**6-31G[10]**	**6-31G(d)**	**6-31+G**	**6-31G(d,p)**
R(1,2)	1.3466	1.3477	1.3549	1.3474	1.3739	1.3699	1.3758	1.3696
R(1,6)	1.4299	1.4326	1.4307	1.4323	1.4288	1.4263	1.4303	1.4261
R(1,17)	1.0719	1.0754	1.0732	1.0757	1.0854	1.0867	1.0857	1.086
R(2,3)	1.4341	1.4359	1.4352	1.4358	1.4329	1.43	1.4343	1.43
R(2,18)	1.0729	1.076	1.0742	1.0763	1.0864	1.0875	1.0868	1.0869
R(3,4)	1.4245	1.4249	1.4282	1.4248	1.4491	1.4452	1.4497	1.4452
R(3,7)	1.3874	1.3894	1.3925	1.3893	1.4036	1.4005	1.4049	1.4004
R(4,5)	1.4341	1.4359	1.4352	1.4358	1.4329	1.43	1.4343	1.43
R(4,8)	1.3874	1.3894	1.3925	1.3893	1.4036	1.4005	1.4049	1.4004
R(5,6)	1.3466	1.3477	1.3549	1.3474	1.3739	1.3699	1.3758	1.3696
R(5,19)	1.0729	1.076	1.0742	1.0763	1.0864	1.0875	1.0868	1.0869
R(6,20)	1.0719	1.0754	1.0732	1.0757	1.0854	1.0867	1.0857	1.086
R(7,10)	1.3874	1.3894	1.3925	1.3893	1.4036	1.4005	1.4049	1.4004
R(7,16)	1.0738	1.0767	1.0752	1.077	1.0873	1.0884	1.0877	1.0877
R(8,9)	1.3874	1.3894	1.3925	1.3893	1.4036	1.4005	1.4049	1.4004
R(8,21)	1.0738	1.0767	1.0752	1.077	1.0873	1.0884	1.0877	1.0877
R(9,10)	1.4245	1.4249	1.4282	1.4248	1.4491	1.4452	1.4497	1.4452
R(9,15)	1.4341	1.4359	1.4352	1.4358	1.4329	1.43	1.4343	1.43
R(10,11)	1.4341	1.4359	1.4352	1.4358	1.4329	1.43	1.4343	1.43
R(11,12)	1.0729	1.076	1.0742	1.0763	1.0864	1.0875	1.0868	1.0869
R(11,13)	1.3466	1.3477	1.355	1.3474	1.3739	1.3699	1.3758	1.3696
R(13,14)	1.4299	1.4326	1.4306	1.4323	1.4288	1.4263	1.4303	1.4261
R(13,22)	1.0719	1.0754	1.0732	1.0757	1.0854	1.0867	1.0857	1.086
R(14,15)	1.3466	1.3477	1.355	1.3474	1.3739	1.3699	1.3758	1.3696
R(14,23)	1.0719	1.0754	1.0732	1.0757	1.0854	1.0867	1.0857	1.086
R(15,24)	1.0729	1.076	1.0742	1.0763	1.0864	1.0875	1.0868	1.0869

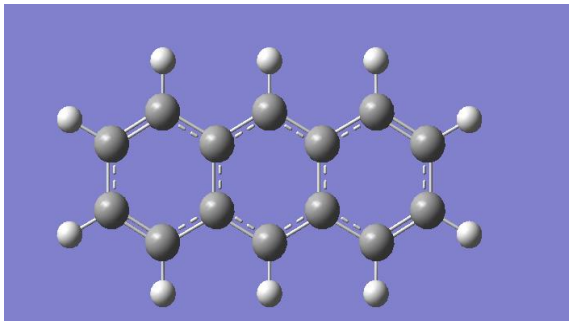

Figure 1: Optimized Structure of Anthracene

Table 1 indicates that at both levels of theory (RHF and DFT), the basis set 6-31G [11] gives the lowest values of the bond lengths and 6-31+G gives the highest values. It is predicted that the bonds R(1,17): C1-H17, R(6,20): C6-H20, R(13,22): C13-H22 and R(14,23): C14-H23 between Carbon and Hydrogen atoms at the indicated positions possess the lowest values of bond lengths ranging from 1.0719Å at RHF/6-31G to 1.0867 Å at B3LYP/6-31G(d). These are the strongest bonds in the Anthracene molecule which cannot be easily broken. On the other hand, R(2,3), R(10,11) and R(9,15) between Carbon-Carbon atoms at the specified positions have the highest values of bond lengths ranging from 1.4341 Å to 1.4159 Å. These are the weakest bonds and are within the benzene rings. However, it is noted that on an average basis, the bond lengths are basically of same strength for all C-H and C-C bonds based on the symmetric nature of anthracene molecule. For C2-C3, C3-C4, and C1-C6 bonds, 2,4,6trinitrotolune; a derivative of Anthracene is predicted to have shorter bond lengths than for Anthracene molecule studied in this work and those in [10]. This could be due to the heavy groups (NO_2, CH_3) attached to C2, C1 and C6 of 2,4,6trinitrotolune. Also, a similar trend is observed in the bond angles (shown in Table 2) at B3LYP/6-31G level of theory [10,11].

Table 2: Optimized Bond Angles (˚)ofAnthracene molecule

Bond Angles	**RHF**				**B3LYP**			
	6-31G[10]	6-31G(d)	6-31+G	6-31G(d,p)	6-31G[10]	6-31G(d)	6-31+G	6-31G(d,p)
A(2,1,6)	120.5026	120.4849	120.4343	120.4925	120.4258	120.4331	120.4028	120.4409
A(2,1,17)	120.4399	120.3348	120.3652	120.3046	120.2436	120.1633	120.23	120.1554
A(6,1,17)	119.0574	119.1803	119.2005	119.2029	119.3307	119.4037	119.3672	119.4037
A(1,2,3)	120.9085	120.9052	120.9398	120.8991	120.9857	120.9729	120.9979	120.9672
A(1,2,18)	120.7818	120.586	120.559	120.5611	120.5779	120.5736	120.5176	120.5633
A(3,2,18)	118.3097	118.5088	118.5012	118.5398	118.4364	118.4535	118.4845	118.4695
A(2,3,4)	118.5889	118.6099	118.6259	118.6084	118.5886	118.5941	118.5993	118.5918
A(2,3,7)	122.1413	122.15	122.1679	122.1369	122.3186	122.3228	122.2988	122.31
A(4,3,7)	119.2698	119.2401	119.2062	119.2547	119.0929	119.0831	119.1018	119.0982
A(3,4,5)	118.5889	118.61	118.626	118.6085	118.5885	118.5941	118.5993	118.5919
A(3,4,8)	119.2697	119.2401	119.2066	119.2547	119.0928	119.0831	119.1018	119.0981
A(5,4,8)	122.1413	122.1499	122.1675	122.1368	122.3187	122.3228	122.2989	122.31
A(4,5,6)	120.9085	120.9051	120.9397	120.8991	120.9856	120.9728	120.9978	120.9672
A(4,5,19)	118.3097	118.5087	118.5005	118.5397	118.4364	118.4535	118.4845	118.4695
A(6,5,19)	120.7818	120.5861	120.5597	120.5612	120.578	120.5737	120.5177	120.5633
A(1,6,5)	120.5026	120.4849	120.4343	120.4924	120.4258	120.4331	120.4029	120.4409
A(1,6,20)	119.0577	119.1805	119.2	119.203	119.3313	119.4043	119.3679	119.4044
A(5,6,20)	120.4397	120.3347	120.3657	120.3046	120.2428	120.1626	120.2292	120.1547
A(3,7,10)	121.4606	121.5199	121.5874	121.4906	121.8144	121.8338	121.7964	121.8037
A(3,7,16)	119.27	119.2403	119.2064	119.2549	119.0931	119.0834	119.1022	119.0985
A(10,7,16)	119.2695	119.2399	119.2063	119.2545	119.0925	119.0828	119.1015	119.0978
A(4,8,9)	121.4606	121.5199	121.5873	121.4906	121.8144	121.8338	121.7964	121.8037
A(4,8,21)	119.2699	119.2403	119.2066	119.2549	119.0932	119.0834	119.1022	119.0985
A(9,8,21)	119.2695	119.2399	119.2061	119.2545	119.0924	119.0828	119.1014	119.0978
A(8,9,10)	119.2697	119.24	119.2062	119.2547	119.0928	119.0831	119.1018	119.0982
A(8,9,15)	122.1413	122.1499	122.1675	122.1368	122.3188	122.3229	122.299	122.3101
A(10,9,15)	118.589	118.6101	118.6263	118.6085	118.5884	118.594	118.5992	118.5917
A(7,10,9)	119.2697	119.24	119.2064	119.2547	119.0928	119.083	119.1018	119.0981
A(7,10,11)	122.1413	122.1499	122.1677	122.1368	122.3186	122.3227	122.2988	122.3099
A(9,10,11)	118.589	118.6101	118.6258	118.6085	118.5887	118.5942	118.5994	118.592
A(10,11,12)	118.31	118.5091	118.5014	118.5401	118.4365	118.4537	118.4847	118.4696
A(10,11,13)	120.9084	120.9051	120.9397	120.899	120.9856	120.9728	120.9978	120.9672
A(12,11,13)	120.7816	120.5858	120.5589	120.5609	120.5779	120.5736	120.5175	120.5632
A(11,13,14)	120.5026	120.4849	120.4344	120.4924	120.4257	120.433	120.4028	120.4409
A(11,13,22)	120.4396	120.3345	120.365	120.3044	120.2432	120.1629	120.2296	120.155
A(14,13,22)	119.0578	119.1806	119.2007	119.2032	119.3311	119.4041	119.3676	119.4041
A(13,14,15)	120.5026	120.4848	120.4341	120.4924	120.4259	120.4331	120.4029	120.441
A(13,14,23)	119.0578	119.1806	119.2007	119.2031	119.331	119.404	119.3676	119.4041
A(15,14,23)	120.4396	120.3346	120.3653	120.3045	120.2431	120.1628	120.2295	120.1549
A(9,15,14)	120.9084	120.9051	120.9397	120.8991	120.9857	120.9728	120.9979	120.9672
A(9,15,24)	118.31	118.509	118.5011	118.54	118.4366	118.4537	118.4848	118.4697
A(14,15,24)	120.7816	120.5859	120.5592	120.561	120.5777	120.5735	120.5174	120.5631

Table 2 predicts that all the bond angles in Anthracene are very close to 120 degrees. The angles with the lowest values area (9,15,24), A(10,11,12) and A(4,5,19) with a value of 118.31˚ at RHF/6-31G. These are all C-C-H angles. C-C-C angles: A(2,3,7), A(5,4,8) and A(7,10,11) with bond angles of 122.1413 ˚ at RHF/6-31G are the highest. Higher values for the bond angles C5-C6-C1, C3-C4-C5 and C1-C2-C3 bond angles are predicted for 2,4,6 trinitrotolune [11] compared to those of the Anthracene Also, a comparative analysis of the optimized parameters (bond angles and lengths) obtained in this study and that of [12] reveal a similar trend. The bond lengths for Anthraquinone and diaminoanthracone are less than that of anthracene at B3LYP level of theory using 6-31G basis set. It is also predicted that the presence of the double oxygen bonds and NH_2 bonds in the derivatives of anthracene has an effect on the bond angles [12].

4.2 Energy Band Gaps

Accurate band gap calculations are of prime importance in determining if reasonable wave front pressures can cause a reduction in the band gap. For comparison, different basis sets have been used and their effect on the band gaps and the molecular highest occupied molecular orbital (HOMO) - lowest unoccupied molecular orbital (LUMO) for Anthraceneis shown in Table 4.

Table 3: Energy Band Gap of Anthracene at Various Levels of Theory

Method		**HOMO(a.u)**	**LUMO (a.u)**	**Eg (a.u)**	**Eg (eV)**
RHF	6-31G	1.13646	1.17702	0.04056	1.1037
	6-31G(d)	1.13600	1.17251	0.03651	0.9935
	6-31+G	1.08198	1.11966	0.03768	1.0254
	6-31G(d,p)	1.13523	1.17195	0.03672	0.9992
B3LYP	6-31G	1.22856	1.32442	0.09586	2.6085
	6-31G(d)	1.22541	1.31844	0.09303	2.5315
	6-31+G	1.21347	1.28747	0.074	2.0137
	6-31G(d,p)	1.22441	1.31738	0.09297	2.5299
Experimental	3.72 ± 0.03eV [13]				

The band gap energies are less than 3eV at all levels of theory for all basis sets. This indicates that the molecule is a very good semi-conductor material. Inclusion of electron correlation increases the values of the band gap and approaches the experimental value. Thus, DFT calculations are more in agreement with the experimental value [13] than the RHF values.

5.0 Conclusion

The significance of computing the optimized structure and energies of Anthracene; a semi-conductor material cannot be over emphasized. Measuring the band gap is important in the semiconductor and nanomaterial industries. The band gap energy of insulators is large (> 4eV), but lower for semiconductors (< 3eV). Our study in this article clearly shows that Anthracene is a very promising organic semi-conductor material.

6.0 References

[1] Berlman I. D. (1973) Energy Transfer Parameters of Aromatic Compounds, Academic Press, New York

[2] Berberan-santos M. N. and Valeur B. (1991) Fluorescence Polarization by Electronic Energy Transfer in Donor- Acceptor Pairs of Like and Unlike Molecules, J. Chem. Phys. 95, 8048–8055

[3] Dguigui K., El Hallaoui M. and Mbarki S. (2012); Ab Initio and DFT Study of Polythiophene Energy Band Gap and Substitutions effects; IJRRAS. 12(3), 427-430

[4] Förster R. (1948); Förster's theory of resonance energy transfer, Photochem. Photobiol. Sci. 7, 1444-1448.

[5] Berlman I. D. (1973) Energy Transfer Parameters of Aromatic Compounds, Academic Press, New York.

[6] Baumann J. and Fayer M. D. (1986) Excitation Energy Transfer in Disordered Two-Dimensional and Anisotropic Three-Dimensional Systems: Effects of Spatial Geometry on Time-Resolved Observables, J. Chem. Phys. 85, 4087-4107.

[7] Frisch M. J, Trucks G W, Schlegel H B, Scuseria G E, Robb M A, Cheeseman J R, Montgomery J A, Vreven Jr T, Kudin K N, Burant J C, Millam M, Iyengar S S, Tomasi J, Barone V, Mennucci B, Cossi M, Scalmani G, Rega N, Petersson G A, Nakatsuji H, Hada M, Ehara M, Toyota K, Fukuda R, Hasegawa J, Ishida M, Nakajima T, Honda Y, Kitao O, Nakai H, Klene M, Li X, Knox J E, Hratchian H P, Cross J B, Adamo C, Jaramillo J, Gomperts R, Stratmann R E, Yazyev O, Austin AJ, Cammi R, Pomelli C, Ochterski J W, Ayala P Y, Morokuma K, Voth G A, Salvador P, Dannenberg J J, Zakrzewski V G, Dapprich S, Danniels A D, Strain M C, Farkas O, Malick D K, Rabuck A D, Raghavachari K, Foresman J B, Ortiz J V, Cui Q, Baboul A G, Clifford S, Cioslowski J, Stefanov B B, Liu G, Liashenko A, Piskorz P, Komaromi I, Martin R L, Fox D J, Keith T, Al-Laham M A, Peng C Y, Nanayakkara A, Challacombe M, Gill PMW, Johnson B, Chen W, Wong M W, Gonzalez C, and Pople J A; Gaussian 03, Revision C.02 (2004)Gaussian, Inc., Wallingford CT, 2004, www.gaussian.com

[8] Becke A.D. (1993), "Density Functional Thermochemistry. III. The role of exact exchange", Journal of Chemical Physics, 98, 5648

[9] Lee C., Yang W. and Parr R.G.(1988), "Development of the Colle-Salvetti correlation-energy formula into a functional of the electron density", Physical Review B, 37, 785

[10] Gurku U. and C. E.Ndikilar (2012), Electronic Structure and Properties of the Organic Semi Conductor Material Anthracene in Gas Phase and Ethanol: An ab initio and DFT Study", The African Review of Physics 7:253 - 263

[11] Clarkson J., Smith W., Batchelder D., Smith D. and Coats A.(2003). "A theoretical study of the structure and vibration of 2,4,6-trinitrotoluene", Journal of Molecular Structure. 648: 203-216

[12] Kukhta A.V., Kukhta I.N., Kukhta N.A., Neyra O.L. and Meza E. (2011). "DFT study of the

electronic structure of anthracene derivatives in their neutral, anion and cation forms" Journal of Physics B, 41, 205701

[13] Vaubel G. and Baesler H. (1968), "Determination of the band gap in Anthracene", Physics Letters A, 27(6): 328-329

7.0 Acknowledgement

We are thankful to the Council of Scientific and Industrial Research (CSIR), India for financial support through Emeritus Professor scheme (Grant No21(0582)/03/EMR-II) to Prof. A.N. Singh of the Physics Department, Bahamas Hindu University, India which enabled him to purchase the Gaussian Software. We are most grateful to Emeritus Prof. A.N. Singh for donating this software to Physics Department, Gombe State University, Nigeria